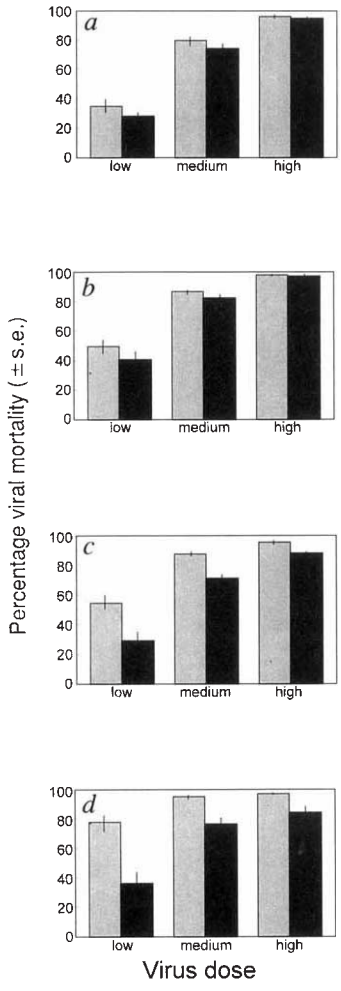

FIG. 3 Percentage virus-induced mortality in wild-type (shaded bars) and recombinant (black bars) treatments at three virus doses, sampled on four occasions: *a*, 2 days; *b*, 7 days; c, 11 days, and *d*, 16 days after release. Error bars are the least significant difference between treatments. Each timepoint was analysed separately. For the first two timepoints, mortality varied between doses (day 2; $F=155.2$; d.f.$=2,20$; $P<0.001$; ANOVA with binomial errors and scale parameter 2.98; day 7; $F=154.8$; d.f.$=2,20$; $P<0.001$, ANOVA with binomial errors and scale parameter 2.39), but mortality did not differ significantly between virus treatments (day 2; $F=3.04$; d.f.$=1,20$; n.s.; ANOVA as above; day 7; $F=3.97$; d.f.$=1$; n.s.; ANOVA as above). However, at days 11 and 16, both virus type and dose were significantly different, with the recombinant virus causing significantly lower mortality (day 11: virus type: $F=30.28$; d.f.$=1,20$; $P<0.01$; dose: $F=73.8$; d.f.$=2,20$; $P<0.01$; Day 16, virus type: $F=41.33$; d.f. 1,20; $p<0.01$; dose: $F=17.29$, d.f. 2,20; $p<0.01$). In each case the analysis is weighted according to the sample size, so allowing for the difference in recovery rates illustrated in Fig. 2.

sprayed inoculum). This variation may be due to differences in the pathology and behaviour of insects infected by the two viruses. Insects infected with wild-type NPV usually remained on the plant after death, where they liquified and thus aided release of large quantities of virus, whereas recombinant infected larvae fell onto the soil and did not lyse. The yield of virus was also reduced in larvae infected with the recombinant (such as 9.6×10^8 polyhedra/larva (C6) and 9.9×10^7 polyhedra/larva (AcST-3) for *T.ni* larva infected as fourth instars), further reducing the likelihood of transmission. Thus the recombinant virus may be less readily transmitted to other larvae, resulting in reduced secondary infection, which, if confirmed, could have important implications for risk assessment. The environmental safety of genetically modified baculoviruses has been discussed[20], particularly regarding host range[21,22]: these results indicate that evaluating the safety of such organisms requires the integration of several factors, including transmissability, environmental persistence and host range to arrive at a full risk assessment.

In summary, we have demonstrated that a genetically improved baculovirus insecticide expressing an insect-selective toxin kills *T.ni* larvae more rapidly in the field than the wild-type virus, resulting in improved crop protection. There was also evidence that secondary transmission was lower in insects treated with recombinant virus. These results highlight the importance of speed of action in achieving reduced crop damage and demonstrate that genetic modification can improve the efficacy of bio-insecticides in the field. □

Received 31 January; accepted 2 June 1994.

1. Bishop, D. H. L., Cory, J. S. & Possee, R. D. in *Release of Genetically Engineered and other Micro-organisms* (eds Fry, J. C. & Day, M. J.) 137–146 (Cambridge Univ. Press, Cambridge, 1992).
2. Bonning, B. C. & Hammock, B. D. *Biotechnol. Genet. Engng Rev.* **10,** 455–489 (1992).
3. Carbonell, L. F., Hodge, M. R., Tomalski, M. D. & Miller, L. K. *Gene* **73,** 409–418 (1988).
4. Merryweather, A. T. *et al. J. gen. Virol.* **71,** 1535–1544 (1990).
5. Martens, J. W. M. *et al. Appl. environ. Microbiol.* **56,** 2764–2770 (1990).
6. Stewart, L. M. D. *et al. Nature* **352,** 85–88 (1991).
7. Tomalski, M. D. & Miller, L. K. *Nature* **352,** 82–85 (1991).
8. McCutchen, B. F. *et al. Bio/Technology* **9,** 848–862 (1991).
9. Maeda, S. *et al. Virology* **184,** 777–780 (1991).
10. Tomalski, M. D. & Miller, L. K. *Bio/Technology* **10,** 545–549 (1992).
11. Ribiero, B. M. & Crook, N. E. *J. Invert. Pathol.* **62,** 121–130 (1993).
12. Maeda, S. *Biochem. biophy. Res. Commun.* **15,** 1177–1183 (1989).
13. Eldridge, R., O'Reilly, D. R. & Miller, L. K. *Biol. Control* **2,** 104–110 (1992).
14. Hammock, B. D., Bonning, B. C., Possee, R. D., Hanzlik, T. N. & Maeda, S. *Nature* **344,** 458–461 (1990).
15. Bonning, B. C. & Hammock, B. D. *Am. Chem. Soc. Symposium Series* **551,** 368–383 (1994).
16. Zlotkin, E. *Insect Biochem.* **13,** 219–236 (1983).
17. De Dianous, S., Hoarau, F. & Rocher, H. *Toxicon* **25,** 411–417 (1987).
18. Herrman, R., Fishman, L. & Zlotkin, E. *Insect Biochem.* **20,** 625–637 (1990).
19. Possee, R. D., Hirst, M. L., Jones, L. D. & Bishop, D. H. L. in *Opportunities for Molecular Biology in Crop Protection* (eds Beadle, D. J., Bishop, D. H. L., Copping, L. G., Dixon, G. K. & Holloman, D. W.) 23–33 (British Crop Protection Council Monograph 55, 1993).
20. Cory, J. S. *Rev. med. Virol.* **1,** 79–88 (1991).
21. Williamson, M. *Nature* **353,** 394 (1991).
22. Hammock, B. *Nature* **355,** 119 (1992).
23. Hunter, F. R., Crook, N. E. & Entwistle, P. F. in *Microbiological Methods for Environmental Biotechnology* (eds Grainger, J. M. & Lynch, J. M.) 323–347 (Society for General Microbiology, Reading, 1984).

ACKNOWLEDGEMENTS. We thank the University of Oxford for use of the field site and R. Broadbent and R. Mackenzie for preparation of the enclosures and T. Bourner and A. Duff for their earlier contribution to the field trial. This work was carried out under consent to release application number 93/R3/2 and DOE and MAFF licences (PHF 272B/235/112; PHF 272C/626/63; experimental permit COP 93/00717).

Correlated neuronal discharge rate and its implications for psychophysical performance

Ehud Zohary, Michael N. Shadlen & William T. Newsome*

Department of Neurobiology, Stanford University School of Medicine, Stanford, California 94305, USA

SINGLE neurons can signal subtle changes in the sensory environment with surprising fidelity, often matching the perceptual sensitivity of trained psychophysical observers[1–10]. This similarity poses an intriguing puzzle: why is psychophysical sensitivity not greater than that of single neurons? Pooling responses across neurons should average out noise in the activity of single cells, leading to substantially improved psychophysical performance. If, however, noise is correlated among these neurons, the beneficial effects of pooling would be diminished[10–12]. To assess correlation within a pool, the responses of pairs of neurons were recorded simultaneously during repeated stimulus presentations. We report here that the observed covariation in spike count was relatively weak, the correlation coefficient averaging 0.12. A theoretical analysis revealed, however, that weak correlation can limit substantially the signalling capacity of the pool. In addition, theory suggests a relationship between neuronal responses and psychophysical decisions which may prove useful for identifying cell populations underlying specific perceptual capacities.

We obtained data from 100 pairs of neurons in the middle temporal visual area (MT, or V5) while three rhesus monkeys viewed random dot patterns presented on a video monitor. Because directionally selective neurons in MT supply signals for discriminating the direction of motion in these displays[10,13–15], this system provides an ideal opportunity to measure correlation within a pool of sensory neurons contributing to psychophysical performance. Action potentials were recorded using a single electrode and a spike sorting device which recognized individual

* To whom correspondence should be addressed.

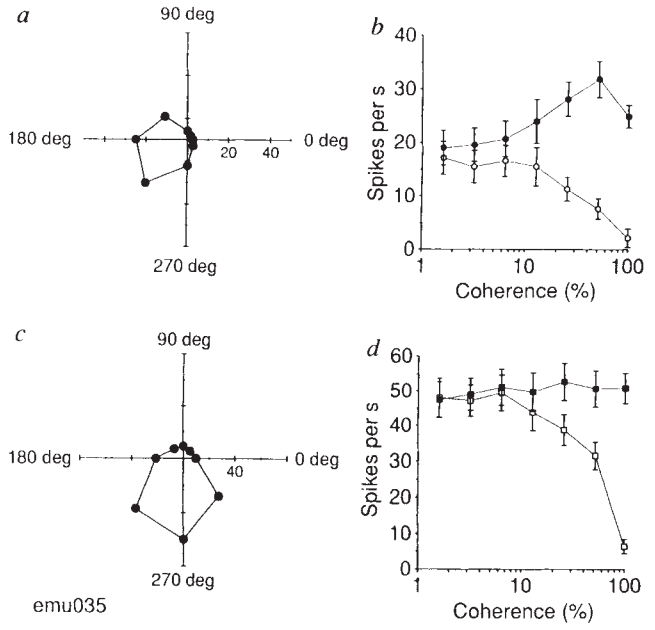

FIG. 1 Average responses of a pair of simultaneously recorded MT neurons during the fixation and discrimination tasks. Polar plots (*a*, *c*) are direction tuning curves measured during the fixation task for neuron 1 (*a*, *b*) and neuron 2 (*c*, *d*). For each data point, the angle indicates the direction of stimulus motion and the distance from the origin represents the average response (spikes per s) to that direction. Coherence–response functions (*b*, *d*) depict average responses to motion signals of increasing strength. Empty symbols indicate responses to preferred direction motion and filled symbols show responses to the opposite (null) direction. Error bars denote standard deviations.

METHODS. Our methods have been described previously[10]. To summarize, direction tuning curves were measured with moving random dot patterns. The position of the dot pattern and the motion speed were set to stimulate the receptive fields of both neurons as well as possible. In the discrimination task, a specified percentage of dots in the visual display moved coherently in one direction while the remaining dots were plotted briefly at random locations, creating a masking motion noise. Monkeys received liquid rewards for reporting the direction of coherent motion correctly. Task difficulty was varied by changing the percentage of dots in coherent motion. On each trial, the direction of motion was either the preferred or null direction of the recorded neurons. If the preferred directions of the two neurons differed substantially, the axis of discrimination was set to the preferred-null axis of the best-responding neuron. In both the discrimination and fixation tasks, each stimulus condition was repeated 10–40 times in random order. Both discrimination and fixation data were obtained for 42 pairs of neurons; fixation data alone were obtained for the remaining pairs.

waveforms using an eight-point template-matching algorithm[16]. We accepted data only from experiments with excellent separation between the two templates and between each template and the background noise.

Responses were recorded during two behavioural tasks, fixation and discrimination. In the former, the monkeys maintained fixation while the visual stimulus was presented within the receptive fields of the two cells. We measured the directional tuning of each neuron and used these data to assess the degree of correlated responsiveness. In the discrimination task, the monkeys reported the direction of coherent motion embedded in a field of random motion noise (see Fig. 1 legend). These data allowed us to assess correlated responsiveness during performance of the discrimination task. Figure 1 illustrates the responses of a pair of MT neurons in the two tasks. Both cells responded selectively to the direction of coherent motion[17], but signalled direction with decreasing reliability as coherent motion was reduced[10].

For each pair, we computed the correlation coefficient, r, between the responses of the two neurons to multiple presentations of a given stimulus. This process was repeated for each stimulus condition tested. Throughout our analyses a response was considered to be the total number of action potentials recorded during presentation of a visual stimulus. A χ^2 test of homogeneity showed that the correlation coefficients computed for a pair of neurons were independent of stimulus condition in 89% of the experiments ($P > 0.05$; correlation coefficients were first transformed to Fisher's z to conform to normality assumptions[18]). Furthermore, we found no systematic difference in the average correlation coefficient between the two behavioural tasks (paired t-test, $P > 0.75$). We therefore combined data across stimulus conditions and tasks to compute a single correlation coefficient for each pair of neurons. To remove the influence of confounding variables such as stimulus strength, spike counts were converted to z-scores using the mean and standard deviation for repetitions of each stimulus type. We then calculated the correlation coefficient between ordered pairs of z-scores.

For the 100 pairs of MT neurons, the mean correlation coefficient was 0.12, a value significantly greater than zero (t-test, $P < 0.0001$). Furthermore, the correlation coefficient depended significantly on the difference in preferred direction of the two neurons. Figure 2*a* shows the distribution of correlation

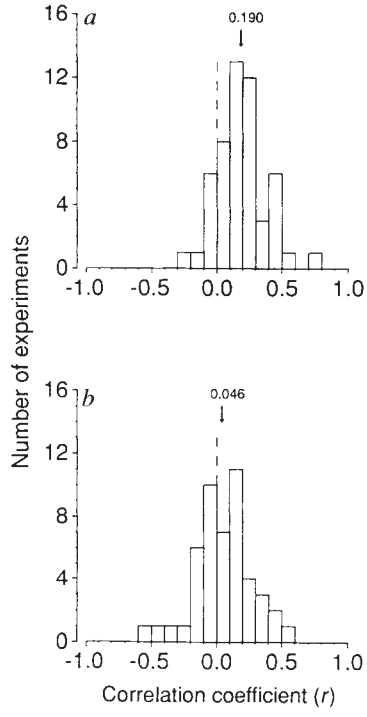

FIG. 2 Frequency histograms of the correlation coefficients measured between pairs of MT neurons. *a*, Distribution of correlation coefficients for 52 pairs of neurons whose preferred directions differed by less than 90°. *b*, Distribution of coefficients for 13 pairs of neurons whose preferred directions differed by more than 90° and 35 pairs for which one neuron was not directional. Three analyses were done to control for artefactual sources of correlated responsiveness. First, we suppressed slow changes in responsiveness by renormalizing the standardized responses in blocks of 20 trials. This manipulation removed any yoked drift in overall responsiveness that might cause spurious correlation between the two neurons, but had no effect on the computed correlation coefficients (paired t-test, $P > 0.9$). To ensure that correlations were not driven entirely by outlier data points (resulting, perhaps, from brief lapses in the quality of isolation), we 'pruned' from each data set trials on which the response of either neuron was more than two standard deviations from that neuron's mean response for a given stimulus condition. Pruning did not affect the correlation coefficients (paired t-test, $P > 0.4$). Last, our random dot patterns typically are computed uniquely on each trial so that the monkey cannot solve the task by memorizing specific patterns of dots for each motion condition. This, however, introduces a small amount of variation among nominally identical stimuli that might give rise to spurious correlation. For four neuronal pairs, therefore, we obtained data using stimuli computed in the usual manner and then using a single predetermined random dot pattern for each stimulus condition (the difference in preferred directions was less than 45° for three pairs and was 103° for the remaining pair). Without stimulus-induced variance, the mean correlation coefficient remained significantly greater than 0 (paired t-test, $P < 0.005$). The correlation coefficients were similar with and without stimulus variation (means =0.15 and 0.22, respectively), although our sample is too small to exclude the possibility of a moderate difference.

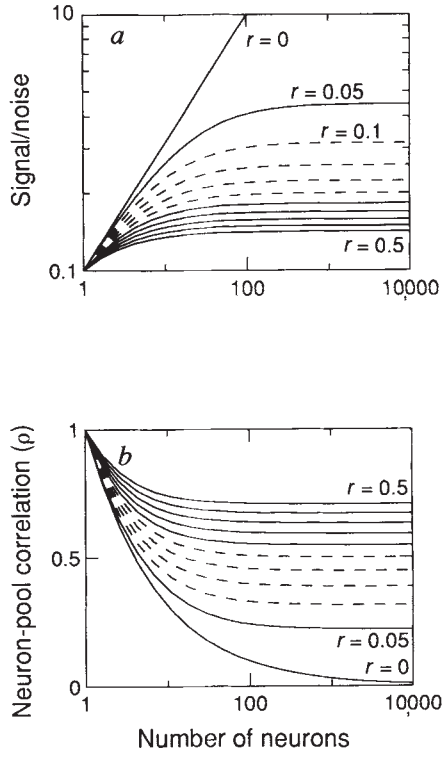

FIG. 3 Effect of pooling for different levels of correlation. *a*, Signal-to-noise ratio of the pooled average response as a function of increasing pool size. *b*, Covariation between individual responses and the pooled average response (ordinate) as a function of increasing pool size (abscissa). Each curve shows results for a particular correlation level within the pool (mean correlation, $\bar{r}=0$ to 0.5 in increments of 0.05). The dashed curves indicate the correlation levels that are most plausible from our physiological data. The curves represent analytical solutions to the equations presented below for M identically distributed neural signals. In the present context, each signal distribution represents the responses of a single neuron contributing to a sensory pool. The assumption of identically distributed signals, while overly simplified from real pools of neurons, is convenient computationally and does not influence our conclusions substantially. For *a*, we calculate the signal-to-noise ratio of M summed signals, $X_1 \ldots X_M$

$$\begin{aligned} \mathrm{S/N} &= \left\langle \frac{\sum_1^M X_i}{\sigma_\Sigma} \right\rangle \\ &= \frac{M\langle X\rangle}{\sqrt{\sum_{i=1}^M \sum_{j=1}^M \mathrm{Cov}\,[X_i, X_j]}} \\ &= \frac{M\langle X\rangle}{\sqrt{M\sigma^2 + M(M-1)\bar{r}\sigma^2}} \end{aligned} \quad (1)$$

where σ_Σ is the standard deviation of the sum and brackets denote expectation. Each curve depicts the S/N of the pool normalized to the S/N of a single neural signal. For large M, improvement is limited by $1/\sqrt{\bar{r}}$. For *b*, we compute the expected correlation, ρ, between one random signal, X_1, and the sum of $X_1 \ldots X_M$. The covariance can be written as

$$\begin{aligned} \rho\sigma_1\sigma_\Sigma &= \rho\sigma\sqrt{\sum_{i=1}^M \sum_{j=1}^M \mathrm{Cov}\,[X_i, X_j]} \\ &= \rho\sigma\sqrt{M\sigma^2 + M(M-1)\bar{r}\sigma^2} \end{aligned} \quad (2)$$

or in terms of products and their expectations

$$\begin{aligned} \mathrm{Cov}\left[X_1, \sum_{i=1}^M X_i\right] &= \left\langle X_1 \sum_{i=1}^M X_i \right\rangle - \langle X_1\rangle \left\langle \sum_{i=1}^M X_i \right\rangle \\ &= \langle X_1^2\rangle + \sum_{i=2}^M \langle X_1 X_i\rangle - M\langle X\rangle^2 \\ &= \sigma^2 + \sum_{i=2}^M \mathrm{Cov}\,[X_1, X_i] \\ &= \sigma^2 + (M-1)\bar{r}_1\sigma^2 \end{aligned} \quad (3)$$

where $\bar{r}_1$ is the average correlation coefficient between signal 1 and each of the other signals. Solving for ρ in equations (2) and (3) we obtain

$$\rho = \frac{1 + (M-1)\bar{r}_1}{\sqrt{M + M(M-1)\bar{r}_1}} \quad (4)$$

The correlation coefficient, ρ, between a single random signal and the sum to which it contributes is plotted in *b*. By analogy with real neuronal pools, this correlation could reflect the covariation between a single neuron's response and the outcome of a psychophysical decision governed by the summed signal, or decision variable. Even with arbitrarily large pools the correlation asymptotes at $\sqrt{\bar{r}_1}$.

coefficients for pairs of neurons whose preferred directions differed by less than 90 degrees, and Fig. 2*b* depicts the corresponding distribution for pairs that failed to meet this condition. The difference between the two distributions is highly significant (*t*-test, $P<0.001$). The correlation values in Fig. 2*a* agree well with similar measurements made in striate cortex of cats[12] and inferotemporal cortex of monkeys[19].

Our data indicate that adjacent MT neurons covary weakly in their response to visual stimuli. Even such weak covariation places fundamental limits on the signal-to-noise ratio (S/N) of any stimulus represented in the activity of a pool of sensory neurons. Figure 3*a* shows the expected improvement in S/N conferred by signal averaging among neuronal pools of increasing size. If neurons within the pool are independent ($r=0$), then S/N should improve by the square root of their number. If neurons within the pool covary even weakly, however, S/N of the pooled response is limited, reaching an asymptote at $r^{-1/2}$ times the S/N of a single neuron in the pool. Note that little increase in S/N is expected for pool sizes larger than 50–100 neurons. Thus, the beneficial effects of pooling are curtailed sharply by weak correlation, rendering more plausible the impressive sensitivity of single neurons relative to psychophysical threshold.

Because our data were recorded from adjacent neurons, we may have overestimated the average correlation in the pool if correlation declines with distance between neurons. Figure 3*a* shows, however, that S/N would reach an asymptotic limit near 100 neurons even if the average correlation within the pool were less than our measured value.

Weak correlation can lead to a covariation between the noisy responses of single neurons and psychophysical decisions. Figure 3*b* illustrates the trial-to-trial correlation expected between the responses of any single neuron and the pooled signals represented in Fig. 3*a*. If neurons within the pool are independent, the covariation of any one neuron with the pooled response must vanish with increasing pool size ($r=0$). If pairs of neurons covary even weakly, however, each neuron retains a covariation with the pooled average even for large pools. If psychophysical decisions are based on pooled signals like those in Fig. 3, near-threshold decisions should be correlated with the response fluctuations of single neurons within the pool.

We have in fact observed such covariation between neuronal responses and psychophysical decisions during performance on our direction discrimination task[20,21], and a similar phenomenon has been reported in the somatosensory system[22]. Our analysis suggests that the covariation of single-neuron responses and psychophysical decisions, an observation that strains credulity at first glance, is a logical consequence of weakly correlated noise within the pool of sensory neurons leading to the decision. If such correlation is a general characteristic of neuronal pools underlying psychophysical performance, trial-to-trial covariation between neuronal responses and decisions may prove useful

for identifying neurons that contribute to various perceptual capacities. □

Received 14 March, accepted 25 May 1994.

1. Mountcastle, V., Talbot, W., Sakata, H. & Hyvarinen, J. *J. Neurophysiol.* **32,** 452–484 (1969).
2. Mountcastle, V., LaMotte, R. & Carli, G. *J. Neurophysiol.* **35,** 122 (1972).
3. Johnson, K., Darian-Smith, I. & LaMotte, C. *J. Neurophysiol.* **36,** 347–370 (1973).
4. Johnson, K., Darian-Smith, I., LaMotte, C., Johnson, B. & Oldfield, S. *J. Neurophysiol.* **42,** 1332–1353 (1979).
5. Tolhurst, D. J., Movshon, J. A. & Dean, A. F. *Vision Res.* **23,** 775–785 (1983).
6. Bradley, A., Skottun, B. C., Ohzawa, I., Sclar, G. & Freeman, R. D. *J. Neurophys.* **57,** 755–772 (1987).
7. Hawken, M. J. & Parker, A. J. in *Vision: Coding and Efficiency* (ed. Blakemore, C.) 103–116 (Cambridge Univ. Press, Cambridge, 1990).
8. Vogels, R. & Orban, G. A. *J. Neurosci.* **10,** 3543–3558 (1990).
9. Recanzone, G. H., Merzenich, M. M. & Schreiner, C. E. *J. Neurophysiol.* **67,** 1071–1091 (1992).
10. Britten, K. H., Shadlen, M. N., Newsome, W. T. & Movshon, J. A. *J. Neurosci.* **12,** 4745–4765 (1992).
11. Johnson, K. *J. Neurophysiol.* **43,** 1793–1815 (1980).
12. van Kan, P., Scobey, R. & Gabor, A. *Expl Brain Res.* **1985,** 559–563 (1985).
13. Newsome, W. T. & Paré, E. B. *J. Neurosci.* **8,** 2201–2211 (1988).
14. Salzman, C. D., Murasugi, C. M., Britten, K. H. & Newsome, W. T. *J. Neurosci.* **12,** 2331–2355 (1992).
15. Murasugi, C. M., Salzman, C. D. & Newsome, W. T. *J. Neurosci.* **13,** 1719–1729 (1993).
16. Worgotter, F., Daunicht, W. & Eckmiller, R. *J. Neurosci. Meth.* **17,** 141–151 (1986).
17. Zeki, S. M. *J. Physiol., Lond.* **236,** 549–573 (1974).
18. Anderson, T. *An Introduction to Multivariate Statistical Analysis* (Wiley, New York, 1958).
19. Gawne, T. & Richmond, B. *J. Neurosci.* **13,** 2758–2771 (1993).
20. Newsome, W. T., Britten, K. H., Movshon, J. A. & Shadlen, M. in *Neural Mechanisms of Visual Perception. Proc. Retina Res. Fdn* (eds Lam, D.M.-K. & Gilbert, C. D.) 171–198 (Portfolio Publishing, The Woodlands, Texas, 1989).
21. Celebrini, S. & Newsome, W. T. *J. Neurosci.* (in the press).
22. Dubner, R., Kenshalo, D. R., Maixner, W., Bushnell, M. C. & Oliveras, J. L. *J. Neurophysiol.* **62,** 450–457 (1989).

ACKNOWLEDGEMENTS. We thank R. T. Born, J. M. Groh and C. D. Salzman for critical comments on the manuscript and J. A. Movshon, K. H. Britten, L. Maloney and S. Klein for helpful advice. The work was supported by the National Eye Institute, the McDonnell-Pew Foundation and the Howard Hughes Medical Institute.

Activation of the cloned muscarinic potassium channel by G protein βγ subunits

Eitan Reuveny*, Paul A. Slesinger*, James Inglese†, Janine M. Morales‡, Jorge A. Iñiguez-Lluhi§, Robert J. Lefkowitz†, Henry R. Bourne‡, Yuh Nung Jan* & Lily Y. Jan*

* Howard Hughes Medical Institute,
and the Departments of Physiology and Biochemistry,
University of California, San Francisco, California 94143, USA
† Howard Hughes Medical Institute,
and the Departments of Medicine and Biochemistry,
Duke University Medical Center, Durham, North Carolina 27710, USA
‡ Department of Pharmacology, University of California,
San Francisco, California 94143, USA
§ Department of Pharmacology,
University of Texas Southwestern Medical Center,
Dallas, Texas 75235, USA

ACETYLCHOLINE released during parasympathetic stimulation of the vagal nerve slows the heart rate through the activation of muscarinic receptors and subsequent opening of an inwardly rectifying potassium channel[1]. The activation of these muscarinic potassium channels is mediated by a pertussis toxin-sensitive heterotrimeric GTP-binding protein (G protein)[2,3]. It has not been resolved whether exogenously applied G_{α}[4,5] or $G_{\beta\gamma}$[6,7], or both, activate the channel. Using a heterologous expression system, we have tested the ability of different G protein subunits to activate the cloned muscarinic potassium channel, GIRK1[8,9]. We report here that coexpression of GIRK1 with $G_{\beta\gamma}$ but not $G_{\alpha\beta\gamma}$ in *Xenopus* oocytes results in channel activity that persists in the absence of cytoplasmic GTP. This activity is reduced by fusion proteins of the β-adrenergic receptor kinase and of recombinant $G_{\alpha i}$–GDP,

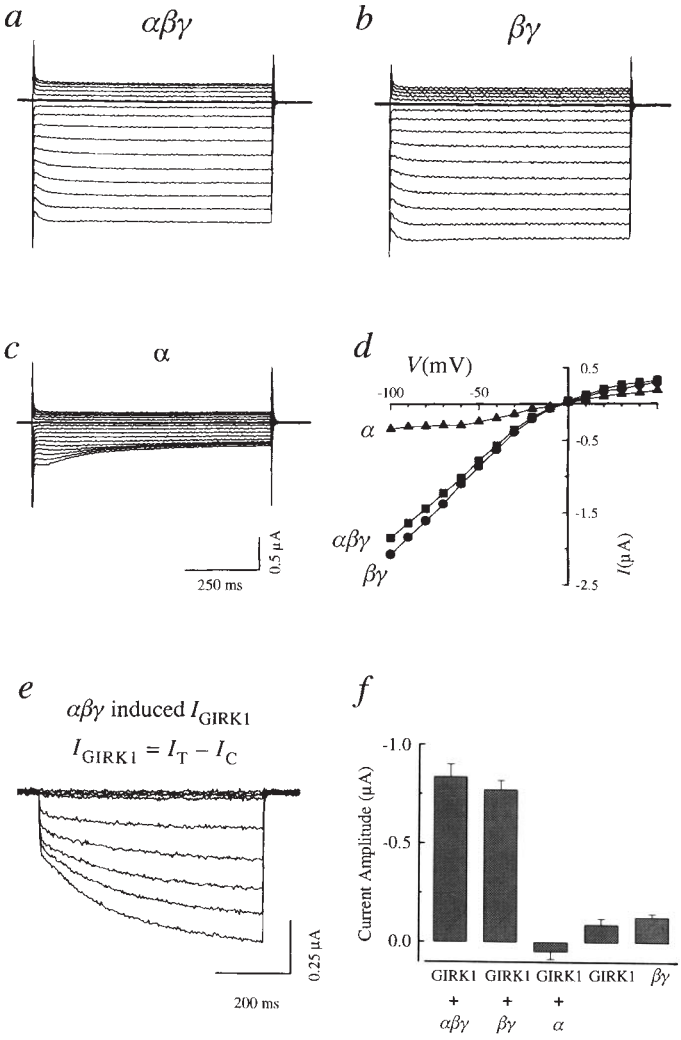

FIG. 1 Coexpression of GIRK1, β1 and γ2 results in channel activation. *a–c*, Inwardly rectifying potassium currents recorded under two-electrode voltage clamp from *Xenopus* oocytes injected with cRNA for GIRK1 and for the various G protein subunit combinations. *a*, αi-2, β1 and γ2; *b*, β1γ2; or *c*, αi-2. The holding potential was 0 mV (the equilibrium potential for potassium, E_K) and current elicited by voltage pulses from −100 to +50 mV in 10 mV increments. *d*, Current–voltage (*I–V*) plot of the steady-state current for traces shown in *a* (■), *b* (●) and *c* (▲). *e*, GIRK1 current induced by αi-2, β1, γ2. In the same batch of oocytes, the average endogenous current present in oocytes injected with only β1, γ2 (I_C, $n = 9$) was subtracted after leak subtraction from the average total current in oocytes produced by coinjecting GIRK1 and αi-2, β1, γ2 (I_T, $n = 9$). Current traces elicited by voltage pulses from +40 to −120 mV in 20 mV increments. *f*, A bar graph of the mean current amplitudes at −100 mV from oocytes injected with cRNA for GIRK1 (−160 ± 43 nA; $n = 3$) or GIRK1 together with αi-2β1γ2 (−836 ± 62 nA; $n = 32$), β1γ2 (−771 ± 47 nA; $n = 39$) or αi-2 (48 ± 38 nA; $n = 14$), or β1γ2 alone (−129 ± 18 nA; $n = 10$). Current amplitudes recorded from oocytes injected with GIRK1 and αi-2β1γ2 or β1γ2 were significantly larger than those from oocytes injected with GIRK1 and αi-2, GIRK1 alone or β1γ2 alone (ANOVA followed by Fisher's least significance difference test (LSD), $P < 0.001$). Assuming a linear leak, the current at +20 mV was scaled and subtracted from the current at −100 mV (measured at the end of the voltage pulse) or a P/−10 protocol was used.

METHODS. Oocytes were isolated as described previously[8], and injected with 50 nl solution containing *in vitro* transcribed (~100 ng μl^{-1}) GIRK1 cRNA, with or without 150 ng μl^{-1} β1γ2 cRNA, and 3′ untranslated region of the *Xenopus* β-globin gene (gift from A. Connolly). Macroscopic currents were recorded at 22–25 °C using two-electrode voltage-clamp as described previously[8]. The bath solution contained 90 mM KCl; 2mM $MgCl_2$; 5 mM HEPES adjusted to pH 7.4 with KOH. Average values are mean ±s.e.m.